Physica B 175 (1991) 187–197
North-Holland

Andreev reflection and the Josephson effect in a quantum point contact

An analogy with phase-conjugating resonators

H. van Houten and C.W.J. Beenakker
Philips Research Laboratories 5600 JA Eindhoven, The Netherlands

We discuss the analogy between the axial mode spectrum of an optical resonator with one or two phase-conjugating mirrors, and the quasiparticle excitation spectrum of an NS or SNS junction (N = normal metal, S = superconductor). As a first application, we consider Andreev reflection at an NS interface for the case that the injector of the current is a quantum point contact. We point out that when the point contact is close to pinch-off quantum interference effects will arise in the current–voltage characteristic, and discuss the relation to the well-known geometrical resonances occurring when a wide tunnel barrier is used as an injector. As a second application, we show that the quantized conductance of a point contact has its counterpart in the stationary Josephson effect. The critical current of a superconducting quantum point contact, short compared to the coherence length, is demonstrated to increase stepwise as a function of its width or Fermi energy, with a universal step height $e\Delta_0/\hbar$.

1. Introduction

In this paper, we give a tutorial introduction and discussion of recent theoretical results [1, 2] concerning transport through point contacts between superconducting regions. In the spirit of this symposium, our contribution has an analogy as its leitmotiv. The analogy [3, 4] is between Andreev reflection [5] and optical phase conjugation [6, 7]. This analogy is not as complete as that between conduction in the normal state and transmission of light [8–11], but it is nevertheless instructive.

The basic theoretical concepts underlying Andreev reflection are reviewed in section 2. In section 3 we introduce optical phase conjugation, and discuss the axial mode spectrum of resonators with two phase-conjugating mirrors, as an analogy to the Andreev spectrum in an SNS junction (S = superconductor, N = normal metal). In section 4 we consider possible new effects in an Andreev reflection experiment with a quantum point contact as an injector. We discuss the relation with the geometrical resonances observed in tunneling experiments on an NS bilayer, which has an analogue in a resonator with one normal and one phase-conjugating mirror. The coupling of transverse modes at the quantum point contact – a diffraction effect – is expected to be important, but has not yet been investigated.

In section 5 we review our recent theoretical work on the stationary Josephson effect in a weak link formed by a superconducting quantum point contact [1]. The critical current of a superconducting quantum point contact which is short compared to the coherence length ξ_0 is predicted to increase stepwise as a function of the width of the point contact. The step height $e\Delta_0/\hbar$ is independent of the properties of the junction, but depends only on the energy gap Δ_0 in the bulk superconductors. This effect is the analogue of the quantized conductance [12, 13] of a quantum point contact in the normal state. The origin of the Josephson effect is the dependence of the excitation spectrum on the phase difference of the superconductors on either side of the junction. The axial mode spectrum in an optical resonator with two phase-conjugating mirrors depends on the phase difference of the laser

0921-4526/91/$03.50 © 1991 – Elsevier Science Publishers B.V. (North-Holland)

beams pumping the mirrors. Such a resonator may therefore be regarded as the optical analogue of a weak link exhibiting the Josephson effect.

2. Andreev reflection

Let us first summarize some basic properties of the excitation spectrum of a bulk superconductor. The quasiparticle excitations of a superconductor are described by the two-component wave function $\Psi = (u, v)$, which is a solution of the Bogoliubov–de Gennes (BdG) equation [14]

$$\begin{pmatrix} \mathcal{H} & \Delta \\ \Delta^* & -\mathcal{H}^* \end{pmatrix} \Psi = \epsilon \Psi . \tag{1}$$

Here $\mathcal{H} = (\boldsymbol{p} + e\boldsymbol{A})^2/2m + V - E_F$ is the single-electron Hamiltonian in the presence of a vector potential $\boldsymbol{A}(\boldsymbol{r})$ and an electrostatic potential $V(\boldsymbol{r})$. The excitation energy $\epsilon > 0$ is measured relative to the Fermi energy E_F. The pair potential $\Delta(\boldsymbol{r})$ vanishes in a normal metal. In this case u and v are the wave functions of independent electron and hole excitations.

The dispersion law for a normal metal in the case $\boldsymbol{A} = 0$, $V = 0$ is given by

$$\epsilon = |p^2/2m - E_F| \sim \hbar v_F |k - k_F| , \tag{2}$$

in terms of momentum p or wave vector k, with $v_F \equiv (2E_F/m)^{1/2}$ the Fermi velocity, and $k_F \equiv mv_F/\hbar$ the Fermi wave vector. The linear approximation in eq. (2) holds if $\epsilon \ll E_F$. A plot of ϵ versus k is given in fig. 1 (dashed curve). The dispersion law corresponds to electron excitations ($v = 0$) for $|k| > k_F$, and to hole excitations ($u = 0$) for $|k| < k_F$.

In a superconductor, Δ is non-zero. The coupled equations for u and v then describe a mixture of electron and hole excitations. Consider a uniform bulk superconductor with $\Delta(\boldsymbol{r}) = \Delta_0 e^{i\phi}$ and $V(\boldsymbol{r}) = 0$. A plane wave solution of the BdG equation has the form

$$\begin{pmatrix} u \\ v \end{pmatrix} = \begin{pmatrix} e^{i\eta/2} \\ e^{-i\eta/2} \end{pmatrix} e^{i\boldsymbol{k}\cdot\boldsymbol{r}} , \tag{3}$$

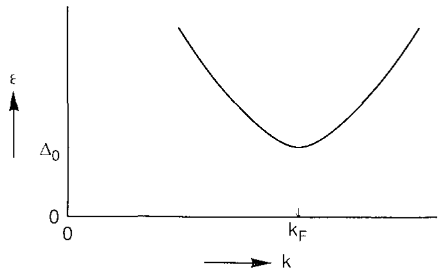

Fig 1 Dispersion relation for electrons and holes in a normal metal (dashed curve) and for quasiparticles in a superconductor, exhibiting an energy gap Δ_0 (full curve)

where η and $k \equiv |\boldsymbol{k}|$ satisfy [15]

$$\epsilon = \Delta_0 \cos(\eta - \phi) ,$$
$$\hbar^2 k^2/2m = E_F + i\Delta_0 \sin(\eta - \phi) . \tag{4}$$

The resulting dispersion law is given by

$$\epsilon = [(\hbar^2 k^2/2m - E_F)^2 + \Delta_0^2]^{1/2} , \tag{5}$$

as plotted in fig. 1 (full curve). Quasiparticles have an excitation gap Δ_0 in a uniform superconductor. For $\epsilon \gg \Delta_0$ the dispersion laws (2) and (5) of normal metal and superconductor coincide.

The (unnormalized) wave functions $\Psi^{e,h}$ describing an electron-like (e) or hole-like (h) quasiparticle at energy ϵ are given by

$$\Psi^{e,h} = \begin{pmatrix} e^{i\eta^{e,h}/2} \\ e^{-i\eta^{e,h}/2} \end{pmatrix} e^{\pm i\boldsymbol{k}^{e,h}\cdot\boldsymbol{r}} , \tag{6}$$

with the definitions*

$$\eta^{e,h} = \phi + \sigma^{e,h} \arccos(\epsilon/\Delta_0) , \tag{7}$$

$$k^{e,h} = (2m/\hbar^2)^{1/2}[E_F + \sigma^{e,h}(\epsilon^2 - \Delta_0^2)^{1/2}]^{1/2} , \tag{8}$$

$$\sigma^e = 1, \quad \sigma^h = -1 . \tag{9}$$

One can verify that for $\epsilon \gg \Delta_0$, Ψ^e has $v = 0$ (a true electron), while Ψ^h has $u = 0$ (a true hole).

* The function arccos t is defined such that arccos $t \in (0, \pi/2)$ for $0 < t < 1$, for $t > 1$, one has i arccos $t = \ln[t + (t^2 - 1)^{1/2}]$

At $\epsilon = \Delta_0$ one has $\Psi^e = \Psi^h$, so that the excitations have equal electron and hole character.

Andreev reflection is the anomalous reflection of an electron with $\epsilon < \Delta_0$ in a normal metal at the boundary with a superconductor [5]. Because of the excitation gap Δ_0, the electron cannot propagate in the superconductor. Ordinary specular reflection has only a small probability if the kinetic energy of motion normal to the NS interface is much larger than Δ_0 (which is the case except for grazing incidence, since $\Delta_0 \ll E_F$). Instead, a Cooper pair is added to the superconductor, the incident electron is annihilated, and a hole is reflected back along the original path of the electron. This is known as Andreev reflection. Incident and reflected quasiparticles have approximately equal wave vectors $k^e \approx k_F + \epsilon/\hbar v_F$ and $k^h \approx k_F - \epsilon/\hbar v_F$, but opposite directions of motion (as follows from the opposite sign of the group velocity $d\epsilon/\hbar\, dk$ for electrons and holes). Energy is conserved: The Cooper pair has energy $2E_F$, the energy of the incident electron is $E_F + \epsilon$, and that of the reflected hole is $E_F - \epsilon$. Momentum is conserved up to terms of order $\hbar|k^e - k^h| \lesssim \hbar/\xi_0$, with $\xi_0 \equiv \hbar v_F/\pi\Delta_0$ the superconducting coherence length.

Andreev reflection can be described by the BdG equation. The variation of $\Delta(\boldsymbol{r})$ at the NS interface has in general to be determined self-consistently from the equation

$$\Delta(\boldsymbol{r}) = g(\boldsymbol{r}) \sum_n v_n^*(\boldsymbol{r}) u_n(\boldsymbol{r})[1 - 2f(\epsilon_n)] . \qquad (10)$$

Here g is the BCS coupling constant ($g = 0$ in N and $g > 0$ in S), f is the Fermi function, and the sum is over all eigenvalues $\epsilon_n > 0$. The qualitative features of Andreev reflection are independent of the precise pair potential profile. Consider, as an example, a step-function profile for the pair potential ($\Delta = 0$ for $z < 0$, and $\Delta = \Delta_0\, e^{i\phi}$ for $z > 0$). In the normal metal ($z < 0$), the incident electron has a wave function $A \exp(i\boldsymbol{k}^e \cdot \boldsymbol{r})(1, 0)$ and the reflected hole has a wave function $B \exp(i\boldsymbol{k}^h \cdot \boldsymbol{r})(0, 1)$. In the superconductor ($z > 0$) only the exponentially decaying wave function $C\Psi^e$ is acceptable if ordinary reflections are neglected. Matching of the amplitudes at $z = 0$ determines the coefficients of the wave functions,

$$A\begin{pmatrix}1\\0\end{pmatrix} + B\begin{pmatrix}0\\1\end{pmatrix} = C\begin{pmatrix}e^{i\eta^e/2}\\ e^{-i\eta^e/2}\end{pmatrix} . \qquad (11)$$

Incident and reflected waves have equal amplitude in absolute value, $|A| = |B|$. The Andreev-reflected hole acquires a phase factor $B/A = \exp(-i\eta^e)$ relative to the incident electron. Similarly, an Andreev-reflected electron acquires a phase factor $\exp(i\eta^h)$. For Andreev reflection at the Fermi energy ($\epsilon = 0$) one has $k^e = k^h$. Only then is the reflected wave the precise time reverse of the incident wave (with a phase difference $-\pi/2 \pm \phi$).

3. Resonators with phase-conjugating mirrors

Andreev reflection is analogous to optical phase conjugation [3]. So far, this analogy has only been worked out for the case of a single NS junction, or a single phase-conjugating mirror [4]. In this paper we consider the bound states that occur due to multiple Andreev reflections in NS bilayers and SNS junctions, and establish the analogy with the axial modes in resonators with normal and/or phase-conjugating mirrors. In the present section we examine the optical problem. For simplicity of notation, we take $\epsilon = \epsilon_0$ for the dielectric constant. Consider a cell of length L_c containing a medium with a third-order nonlinear susceptibility $\chi^{(3)}$, pumped by two intense counter-propagating laser beams of frequency ω_0 (fig. 2(a)). Due to the nonlinear interaction, a weak probe beam of frequency $\omega_0 + \delta$ incident on this medium at $z = -L_c$ emerges amplified at $z = 0$. In addition, a fourth beam is generated, with a wave vector opposite to that of the probe beam. This reflected beam starts with zero intensity at $z = 0$ and emerges from the cell at $z = -L_c$. This is known as four-wave mixing [6, 7]. If $\delta = 0$ (degenerate case) the retro-reflected beam is the exact phase conjugate of the probe beam, except for a different intensity. For non-zero $\delta \ll \omega_0$ (nearly-degenerate four-wave mixing) the

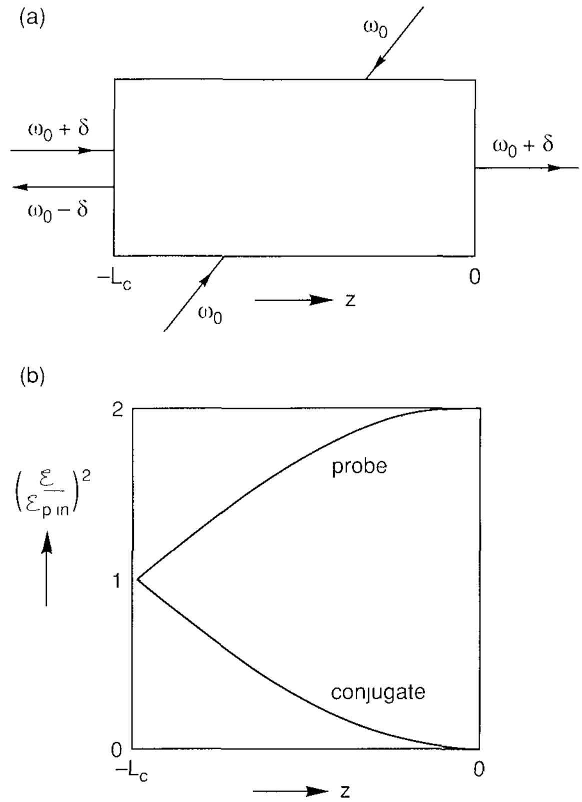

Fig. 2. (a) Four-wave mixing cell pumped by two counter-propagating beams at frequency ω_0, with probe beam at $\omega_0 + \delta$ and a reflected conjugate beam at $\omega_0 - \delta$. (b) Spatial variation of the intensities of probe and conjugate beams within the cell, for $\delta = 0$ and $\kappa_0 L_c = \pi/4$.

reflected beam has frequency $\omega_0 - \delta$, analogous to Andreev reflection as a hole with energy $E_F - \epsilon$ of an incident electron with energy $E_F + \epsilon$. The mechanism of four-wave mixing is that from each of the two pump beams a photon is annihilated. One photon is added to the probe beam, and another to the reflected beam. The frequencies are only approximately equal, to order δ. Hence the requirement $\delta \ll \omega_0$, similar to the case of Andreev reflection. A difference with Andreev reflection is that the wave vector changes sign with four-wave mixing, but not with Andreev reflection.

In order to explore these similarities and differences it is instructive to consider the mathematical description of nearly-degenerate four-wave mixing. This may be done on the basis of a "Schrödinger equation for light" [8], extended to account for the third-order nonlinear susceptibility [4]. In its stationary form, this equation relates the complex amplitudes $\mathcal{E}_p$ and $\mathcal{E}_c$ of the probe beam and its phase-conjugate

$$\begin{pmatrix} H & \gamma^* \\ -\gamma & -H \end{pmatrix}\begin{pmatrix}\mathcal{E}_p \\ \mathcal{E}_c^*\end{pmatrix} = \hbar\delta \begin{pmatrix}\mathcal{E}_p \\ \mathcal{E}_c^*\end{pmatrix}, \qquad (12)$$

where $H \equiv p^2/2m_0 - \frac{1}{2}\hbar\omega_0$. A common factor $e^{-i\omega_0 t}$ has been eliminated from all amplitudes. The equivalent mass of the photon is $m_0 \equiv \hbar\omega_0/c^2$. The probe beam is coupled to its phase conjugate in a region with non-zero γ, which plays the role of the complex pair potential Δ in the superconductor. The strength of the coupling

$$\gamma = \frac{\hbar\omega_0 c}{2\epsilon_0}\,\chi^{(3)}\mathcal{E}_1\mathcal{E}_2\,, \qquad (13)$$

is proportional to the product of the complex amplitudes $\mathcal{E}_1$ and $\mathcal{E}_2$ of the two pump beams with opposite wave vector. Equation (12) is valid only for $\delta \ll \omega_0$, in view of the slowly-varying envelope approximation on which it is based.

For *degenerate* four-wave mixing ($\delta = 0$), the solution in a medium with constant $\gamma = \gamma_0 e^{i\phi}$, for a probe beam traveling in the positive z-direction, is given by

$$\begin{pmatrix}\mathcal{E}_p \\ \mathcal{E}_c^*\end{pmatrix} = \text{constant}\begin{pmatrix}\cos(\kappa_0 z)\,e^{-i\phi/2} \\ -i\sin(\kappa_0 z)\,e^{i\phi/2}\end{pmatrix} e^{ik_0 z}\,, \qquad (14)$$

with $\kappa_0 \equiv \gamma_0/\hbar c$ and $k_0 \equiv \omega_0/c$. The probe beam impinges on the cell at $z = -L_c$ with amplitude $\mathcal{E}_{p\,in}$, and emerges at $z = 0$ with the larger amplitude $\mathcal{E}_{p\,out}$. The conjugate beam starts with zero amplitude at $z = 0$ and emerges with amplitude $\mathcal{E}_{c\,out}$ at $z = -L_c$. The incident amplitude $\mathcal{E}_{p\,in}$ determines the constant prefactor in (14), with the result

$$\mathcal{E}_p(z) = \mathcal{E}_{p,in}\frac{\cos(\kappa_0 z)}{\cos(\kappa_0 L_c)}\exp(ik_0(L_c + z))\,,$$

$$\mathcal{E}_c^*(z) = \mathcal{E}_{p\,in}\frac{\sin(\kappa_0 z)}{\cos(\kappa_0 L_c)} \times \exp\left(i\left[k_0(L_c + z) + \phi - \frac{\pi}{2}\right]\right). \qquad (15)$$

The spatial variation in the cell of the probe and conjugate beam intensities is plotted in fig. 2(b) for a coupling strength $\kappa_0 L_c = \pi/4$, chosen in order to have a conjugate beam with the same intensity as the incident probe beam (i.e. $|\mathscr{E}_{c\ out}|^2 = |\mathscr{E}_{p\ in}|^2$). This choice corresponds most closely to Andreev reflection. The wavelength $2\pi/\kappa_0 \equiv hc/\gamma_0$ is the analogue of the superconducting coherence length $\xi_0 \equiv \hbar v_F/\pi\Delta_0$. These lengths set the scale for the penetration depth in the four-wave mixing cell and in the superconductor, respectively.

Let us now consider *nearly-degenerate* four-wave mixing [16, 17]. Substitution of $(\mathscr{E}_p, \mathscr{E}_c^\dagger) = (e^{i\eta/2}, e^{-i\eta/2})\, e^{i(k_0+\beta)z}$ into eq. (12), with $\gamma = \gamma_0 e^{i\phi}$ and $k_0 = \omega_0/c$, gives a set of equations similar to eq. (4):

$$\hbar\delta = -i\gamma_0 \sin(\eta + \phi)\,,$$

$$\hbar c\beta = -\gamma_0 \cos(\eta + \phi)\,. \tag{16}$$

The dispersion relation following from eq. (16) is

$$\beta = [(\delta/c)^2 + \kappa_0^2]^{1/2}\,, \tag{17}$$

which should be compared to eq. (5). As seen from the plot of the dispersion relation in fig. 3, in the four-wave mixing cell there is a *momentum* gap $\hbar\kappa_0 = \gamma_0/c$, instead of the *energy* gap Δ_0 in the superconductor [4].

The solution in the four-wave mixing cell

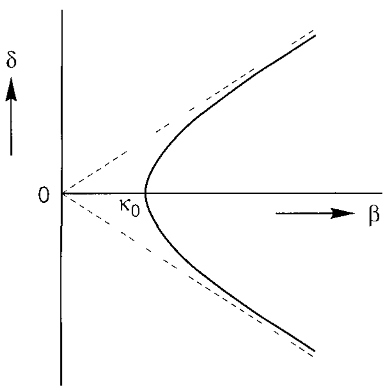

Fig. 3 Dispersion relation for photons in free space (dashed curve) and in a four-wave mixing cell, exhibiting a momentum gap $\hbar\kappa_0$ (full curve)

($|z| < L_c$), for a probe beam moving in the z-direction is of the form

$$\begin{pmatrix} \mathscr{E}_p \\ \mathscr{E}_c^\dagger \end{pmatrix} = A_+ \begin{pmatrix} e^{i\eta_1/2} \\ e^{-i\eta_1/2} \end{pmatrix} e^{i(k_0+\beta)z} + A_- \begin{pmatrix} e^{i\eta_2/2} \\ e^{-i\eta_2/2} \end{pmatrix} e^{i(k_0-\beta)z}\,, \tag{18}$$

where η_1 and η_2 are the two solutions of eq. (16):

$$\eta_1 = -\phi + \pi - \arcsin\left(\frac{i\hbar\delta}{\gamma_0}\right)\,, \tag{19}$$

$$\eta_2 = -\phi + \arcsin\left(\frac{i\hbar\delta}{\gamma_0}\right)\,. \tag{20}$$

The coefficients A_+ and A_- are determined from the requirements $\mathscr{E}_p = \mathscr{E}_{p\ in}$ at $z = -L_c$ and $\mathscr{E}_c = 0$ at $z = 0$. The result is

$$\mathscr{E}_p(z) = \mathscr{E}_{p\ in} \frac{\Omega(z)}{\Omega(-L_c)} \exp(ik_0(L_c + z))\,,$$

$$\mathscr{E}_c^\dagger(z) = \mathscr{E}_{p\ in} \frac{\sin(\beta z)}{\Omega(-L_c)} \times \exp\left(i\left[k_0(L_c + z) + \phi - \frac{\pi}{2}\right]\right)\,, \tag{21}$$

with the definition

$$\Omega(z) \equiv [1 + (\hbar\delta/\gamma_0)^2]^{1/2}\cos(\beta z) + i(\hbar\delta/\gamma_0)\sin(\beta z)\,. \tag{22}$$

For $\delta = 0$ this solution reduces to eq. (15).

A probe beam at frequency $\omega_0 \pm \delta$ ($0 < \delta \ll \omega_0$) generates a reflected beam at frequency $\omega_0 \mp \delta$, with an amplitude

$$\mathscr{E}_{c,out}^\dagger = \mathscr{E}_{p\ in} R\, e^{i\chi^\pm}\,. \tag{23}$$

The phase shift $\chi^\pm$ and the reflection coefficient R follow from the above solution (21). The phase shift between probe and incident beam is given by

$$\chi^\pm = \phi - \frac{\pi}{2} - \arg\Omega(-L_c) \tag{24}$$

$$= \phi - \frac{\pi}{2} \pm \arctan\left[\frac{\Delta k}{2\beta}\tan(\beta L_c)\right]\,, \tag{25}$$

with $\Delta k \equiv 2\delta/c$. Whereas Andreev reflection occurs with (approximately) unit probability for $\epsilon < \Delta_0$, the reflection coefficient R for a four-wave mixing cell depends on the detuning δ,

$$R^2 = \frac{\kappa_0^2 \sin^2(\beta L_c)}{\kappa_0^2 \cos^2(\beta L_c) + (\Delta k/2)^2} . \tag{26}$$

In fig. 4 we have plotted R^2 for $\kappa_0 L_c = \pi/4$. In the weak coupling limit [7] $\kappa_0 \ll |\Delta k|$ the reflection coefficient may be approximated by $R = \kappa_0 L_c \,\mathrm{sinc}(\Delta k L_c/2)$, and the phase shift by $\chi^{\pm} = \phi - \pi/2 \pm \Delta k L_c/2$. In the opposite limit $|\Delta k| \ll \kappa_0$ one has instead $R = 1$ and $\chi^{\pm} = \phi - \pi/2$. As discussed by Siegman et al. [18], the characteristic shape of the R versus Δk curve (reminiscent of the Fourier power spectrum of a square pulse) can be understood from the fact that the interaction time of probe and conjugate beams with the medium is cut off for times exceeding twice the transit time L_c/c. Indeed, the width of the central lobe in fig. 4 corresponds to a detuning $\delta \equiv c\,\Delta k/2 \sim c/L_c$.

In order to establish the analogy with the geometrical resonances in an NS bilayer, and with the Josephson effect in an SNS junction, we examine the axial mode spectrum of an optical resonator. If the resonator is formed by two conventional flat mirrors separated by a distance L (a Fabry–Perot resonator) the axial modes for normal incidence have frequencies

$$\omega_m = m\pi c/L , \quad m = 1, 2, \ldots . \tag{27}$$

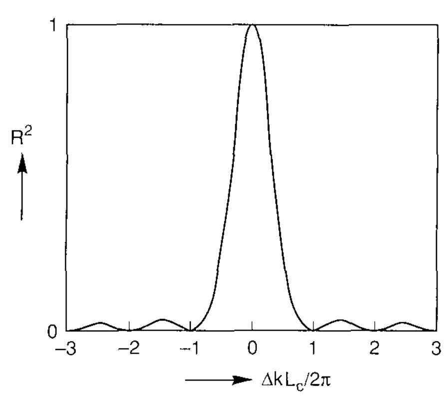

Fig. 4. Power reflection coefficient versus detuning in a four-wave mixing cell, for the case $\kappa_0 L_c = \pi/4$.

This follows from the requirement that the phase shift $2kL$ on a single round trip (including two phase shifts of π on reflection off a front-silvered mirror) is an integer multiple of 2π.

Axial modes may also be formed in a resonator with one conventional mirror and one phase-conjugating mirror (see fig. 5(a)). Because the frequency of probe and conjugate beam jumps by an amount $\pm 2\delta$ on each reflection, the phase shift acquired on *two* round trips should equal an integer multiple of 2π (after which the original frequency is recovered) [17, 18]. In view of eq. (25) this implies an axial mode spectrum which for normal incidence is given by

$$\frac{4\delta L}{c} + 2 \arctan\left[\frac{\Delta k}{2\beta} \tan(\beta L_c)\right] = 2\pi m , \quad m = 0, 1, 2, \ldots . \tag{28}$$

Interestingly, a bound state with frequency ω_0 (i.e. $\delta = 0$, $m = 0$) exists for all values of the resonator length L. As will be discussed in sec-

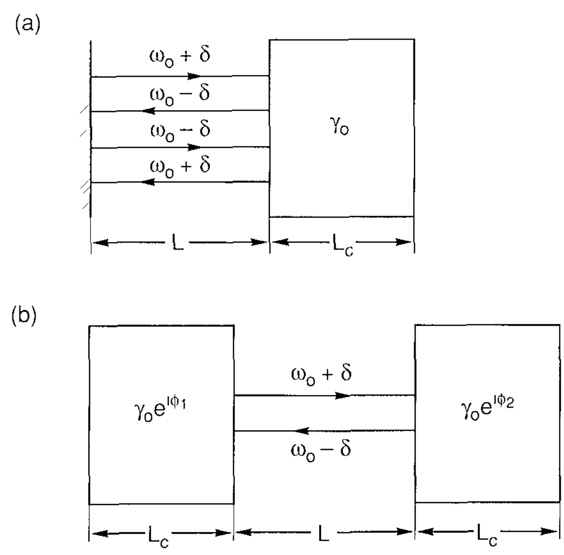

Fig. 5. (a) Optical resonator with one conventional mirror and one phase-conjugating mirror. The criterion for the formation of an axial mode is that the phase shift acquired on two round trips is an integer multiple of 2π. (b) Optical resonator with two phase-conjugating mirrors. The criterion for the formation of an axial mode is that the phase shift acquired on one round trip is an integer multiple of 2π. The mode frequencies depend on the phase difference $\phi_1 - \phi_2$.

tion 4, this axial mode spectrum is analogous to the quasiparticle excitation spectrum in an NS bilayer In the weak coupling limit $\kappa_0 \ll |\Delta k|$ eq (28) reduces to $\delta = m\pi c/[L_c + 2L]$, and in the opposite limit to $\delta = m\pi c/2L$

In a cavity with two phase-conjugating mirrors pumped at the same frequency ω_0, the frequency jumps from $\omega_0 + \delta$ to $\omega_0 - \delta$ and back in a *single* round-trip (see fig 5(b)) [18] The condition for the formation of an axial mode now becomes

$$\frac{2\delta L}{c} \pm \Delta\phi + 2\arctan\left[\frac{\Delta k}{2\beta}\tan(\beta L_c)\right] = 2\pi m \,, \tag{29}$$

where the ± sign corresponds to the two possible propagation directions of the beam with frequency $\omega_0 + \delta$, and $\Delta\phi$ denotes the difference in phase of the coupling constants γ in the two mirrors One may adjust $\Delta\phi$ by varying the phase difference of the pump beams In the weak and strong coupling limits one has $\delta = (\mp\Delta\phi + m2\pi)c/2(L_c + L)$ and $\delta = (\mp\Delta\phi + m2\pi)c/2L$, respectively In either limit the frequency depends linearly on $\Delta\phi$ Note that the difference between the two limits disappears altogether for a short cell with $L_c \ll L$

The discrete excitation spectrum of a clean SNS junction, to be discussed in section 5, has a similar dependence on the phase difference of the pair potential in the two superconducting regions The analogy is most complete for the case $\kappa_0 L_c = \pi/4$, corresponding to a unit reflection probability for $\delta = 0$ In the optical case, there is then at least one axial mode within the first lobe of the reflection probability curve (fig 4), even in the short resonator limit $L \ll L_c$ This is analogous to the fact that an SNS junction has at least one bound state, even in the limit of a very short normal region ($L \ll \xi_0$) The phase dependence of these bound states is at the origin of the Josephson effect

A resonator with two phase-conjugating mirrors does not have stable axial modes if the mirrors are pumped at different frequencies ω_1 and ω_2 The frequency of a wave in the resonator then increases (or decreases) by $2(\omega_1 - \omega_2)$ on each round trip [18] In view of the analogous role of the pumping frequency and the Fermi level in a superconductor, one would expect a similar effect in a voltage biased SNS junction This is indeed the case ϵ increases by eV on each pass through the normal region, until the quasiparticle escapes into the superconductor (when $\epsilon > \Delta_0$) or until inelastic scattering interrupts the process [19]

4. Andreev reflection through a quantum point contact

In a typical Andreev reflection experiment (see fig 6), a point contact in a normal metal is used to inject electrons ballistically towards an interface with a superconductor The Andreev-reflected holes may be detected by focusing them onto a second point contact by means of a magnetic field [20, 21] The application of a magnetic field also leads to a reduction of the conductance of the injector point contact [22, 23], for the following reason The injected electrons are Andreev reflected as holes, back through the point contact (normal reflection can be ignored if there is no potential barrier at the NS interface) Since the charge of the holes is $+e$, Andreev reflection doubles the current and hence the conductance The conductance is reduced to its normal value in a weak magnetic field, because the Andreev-reflected holes are deflected away from the injector (dashed trajectory in fig 6) The reduction of G by a magnetic field is a sensitive probe of Andreev reflection

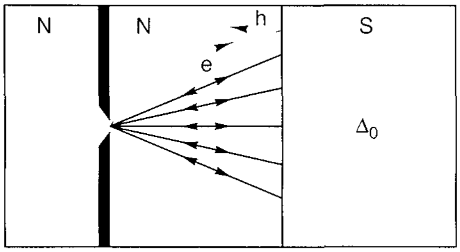

Fig 6 Andreev reflection as holes of electrons which are injected by a point contact (full lines) has the effect of doubling its conductance This effect is suppressed in a magnetic field due to the curvature of the trajectories of electrons and holes (dashed curve)

If the width of the point contact is comparable to the Fermi wavelength λ_F, we have what is known as a *quantum point contact* [11–13]. The conductance of a quantum point contact is quantized in units of $2e^2/h$, $G = N(2e^2/h)$. The integer N equals the number of transverse modes at the Fermi energy which can propagate through the constriction. The conductance of a quantum point contact will also be doubled by Andreev reflection. This should be observable as a quantization of the conductance in units $4e^2/h$, instead of $2e^2/h$.

In between conductance plateaux deviations from the simple factor-of-two enhancement should be expected, however. In particular, if the point contact is small compared to λ_F, ballistic transport is no longer possible, because there are no propagating modes ($N = 0$). The current is then carried by evanescent modes, which can tunnel through the constriction. The problem resembles that of tunneling through a *wide* barrier into a normal metal overlayer on a superconductor (S). In that case the tunnel current can be obtained from the excitation spectrum in the normal metal [23, 24]. The combination of Andreev reflection at the NS interface and normal reflection at the tunnel barrier, gives rise to the formation of bound states for energies $\epsilon < \Delta_0$ [25–27]. This discrete spectrum can be readily obtained for the case of a stepwise increase of the pair-potential at the NS interface, and for specular reflection at the tunnel barrier. The quantization condition is that the phase shift ζ after two Andreev reflections and two specular reflections equals an integer multiple of 2π (see fig. 7(a)). The reflections themselves contribute $\eta^h - \eta^e = -2\arccos(\epsilon/\Delta_0)$ to ζ (cf. eq. (4)). The two "round trips" contribute $2L\delta k/\cos\theta$, with L the separation of tunnel barrier and NS interface, and $\delta k = k^e - k^h$ the wave vector difference of electron and hole. Since $\delta k \sim 2\epsilon/\hbar v_F$ (section 2), one finds the condition for a bound state in the form [25]

$$\zeta \equiv \frac{4\epsilon L}{\hbar v_F \cos\theta} - 2\arccos\frac{\epsilon}{\Delta_0} = 2\pi m\,, \quad m = 0, 1, 2, \ldots . \tag{30}$$

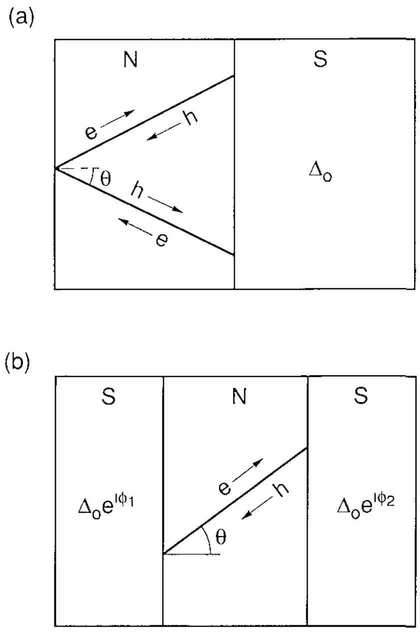

Fig 7 (a) Andreev levels are formed in an NS bilayer if the phase shift acquired on two round trips is an integer multiple of 2π (b) Andreev levels are formed in an SNS junction if the phase shift acquired on one round trip is an integer multiple of 2π The energies of the bound states depends on the phase difference $\phi_1 - \phi_2$.

The spectrum (30) for $\theta = 0$ is similar to that of eq. (28) for a resonator with one phase-conjugating mirror.

The bound states given by eq. (30) are observable as "geometrical resonances" in the differential conductance of a tunnel barrier on top of an NS bilayer [23–27]. The enhancement factor of the current on resonance over its value in the absence of Andreev reflection greatly exceeds the factor of two characteristic of the ballistic case. (The enhancement is similar to the enhancement of the current in resonant tunneling through a symmetric double-barrier tunneling diode.) Calculations of the transmission probability [23, 24] give for $\theta = 0$, $\epsilon < \Delta_0$ the result [24]

$$T(\epsilon) = \frac{2}{1 + s[1 - \cos\zeta]}\,, \tag{31}$$

where s is a function of the transmission probability T_0 of the tunnel barrier in the absence of Andreev reflection As expected, transmission maxima with $T = 2$ are obtained at $\zeta = 2\pi m$ In that case a bound state coincides with the energy of the injected particles (for $\theta = 0$) A tunnel barrier corresponds typically to $T_0 \ll 1$ In that case $s = 2/T_0^2$ [24], so that the minimal transmission is $T = T_0^2/2$ Ballistic transmission corresponds to $T_0 = 1$ Then $s = 0$ [24], so that $T = 2$, independent of the phase ζ

In the case of tunneling through a wide barrier, the transverse modes (corresponding to different values of θ) may be considered independently, since the momentum parallel to the barrier is conserved In contrast, a pinched-off quantum point contact excites a coherent superposition of the transverse modes in the wide normal region [9] * This diffraction effect may well modify the geometrical resonances

5. Josephson effect in a quantum point contact

It is well known that the critical current of a superconducting weak link is determined by its normal-state conductance [28] What happens if the weak link is a quantum point contact? We have recently addressed that question [29] theoretically [1] We find that in a *short* quantum point contact (of length $L \ll \xi_0$) each propagating transverse mode contributes $e\Delta_0/\hbar$ to the critical current at zero temperature As a result, the critical current is predicted to increase stepwise as a function of width or Fermi energy The step height $e\Delta_0/\hbar$ depends on the gap in the bulk superconductors, but not on the properties of the constriction This is to be contrasted with the case of a quantum point contact in an SNS junction with $L_N \gg \xi_0$ where no such universal behavior is found [2] (L_N is the separation of the NS interfaces)

In order to understand the difference between the two geometries, let us first consider the case of an SNS junction without a quantum point contact (fig 7(b)) The pair potential profile has to be determined self-consistently As a first approximation, we assume

$$\Delta(r) = \begin{cases} \Delta_0 \, e^{i\phi_1} & \text{if } z < 0 \,, \\ 0 & \text{if } 0 < z < L_N \,, \\ \Delta_0 \, e^{i\phi_2} & \text{if } z > L_N \end{cases} \tag{32}$$

The bound states for $\epsilon < \Delta_0$ may be found by equating the phase shift acquired on a single round trip to an integer multiple of 2π The resulting condition is [5, 30]

$$\frac{2\epsilon L_N}{\hbar v_F \cos\theta} - 2 \arccos \frac{\epsilon}{\Delta_0} \pm \delta\phi = 2\pi m \,, \quad m = 0, 1, \ldots \,, \tag{33}$$

where $\delta\phi \equiv \phi_1 - \phi_2 \in (-\pi, \pi)$ and θ is the angle with the normal to the N–S interface The $\pm$ sign corresponds to the two directions of motion of the electron (or hole) For $\epsilon \ll \Delta_0$ the spectrum depends linearly on $\delta\phi$, according to $\epsilon = [(2m+1)\pi \mp \delta\phi]\hbar v_F \cos\theta / 2L_N$ Note the similarity to the phase dependence of the axial modes in a resonator with two phase conjugating mirrors (compare with eq (29) in the limit $\Delta k \ll \kappa_0$)

For $L_N \gg \xi_0$ the energy spectrum of the SNS junction depends sensitively on L_N The Josephson current is a piecewise linear function of $\delta\phi$ with a critical current given by [31] $I_c = \alpha G \hbar v_F / eL_N$ where α is a numerical coefficient of order unity (dependent on the dimensionality of the system) and G is the normal state conductance of the SNS junction The dependence of I_c on the junction geometry (through L_N) is characteristic of the case $L_N \gg \xi_0$, and persists if the SNS junction contains a constriction in the normal region [2]

In the opposite limit $L_N \ll \xi_0$, only a single bound state for each of the N transverse modes remains, at energy $\epsilon = \Delta_0 \cos(\delta\phi/2)$ independent of L_N This result implies a zero-temperature Josephson current**

* An atomically sharp tip of a scanning tunneling microscope is likely to function in the same way providing an alternative experimental system in which to study these effects

** The equality $I(\delta\phi) = -N(2e/\hbar)(d\epsilon/d\delta\phi)$ follows from the general formula $I = (2e/\hbar)\, dF/d\delta\phi$ with F the free energy [32] in the limit $T = 0$ $L_N \ll \xi$ [33]

$$I(\delta\phi) = -N \frac{2e}{\hbar} \frac{d\epsilon}{d\delta\phi}$$

$$= N \frac{e}{\hbar} \Delta_0 \sin(\delta\phi/2)\,, \quad \pi < \delta\phi < \pi\,, \qquad (34)$$

and critical current

$$I_c = N \frac{e}{\hbar} \Delta_0\,, \qquad (35)$$

both of which are independent of L_N. The results (34) and (35) are, however, *not* independent of the ansatz (32) made for the pair potential profile, and are therefore only a first approximation to the result for a self-consistent pair potential. The self-consistency equation (10) implies that $\Delta(\boldsymbol{r})$ becomes a constant $\Delta_0\,e^{i\phi}$ only at a distance ξ_0 from the interface with the normal metal, in disagreement with the ansatz (32).

The case of a superconducting quantum point contact is fundamentally different [1]. If the two superconducting reservoirs are coupled via a narrow constriction, of length $L \ll \xi_0$, then non-uniformities in $\Delta(\boldsymbol{r})$ decay on the length scale L rather than ξ_0. This "geometrical dilution" effect was pointed out by Kulik and Omel'yanchuk [34]. The behavior of $\Delta(\boldsymbol{r})$ within the constriction depends on its shape, and on whether the point contact consists of a superconductor or of a normal metal. However, as we have shown in ref. [1], the energy spectrum and Josephson current are independent of the behavior of $\Delta(\boldsymbol{r})$ for $|x| < L$. The results for a superconducting quantum point contact are formally identical to those for an SNS junction with $L_N \ll \xi_0$. However, now the energy spectrum and critical current are the correct results for the self-consistent pair potential, rather than a first approximation. At finite temperatures we find for the Josephson current the expression

$$I(\delta\phi) = N \frac{e}{\hbar} \Delta_0(T) \sin(\delta\phi/2) \times \tanh\left(\frac{\Delta_0(T)}{2k_B T} \cos(\delta\phi/2)\right), \qquad (36)$$

plotted in fig. 8 for three temperatures. In the classical limit $N \to \infty$ our result agrees with that of Kulik and Omel'yanchuk [34].

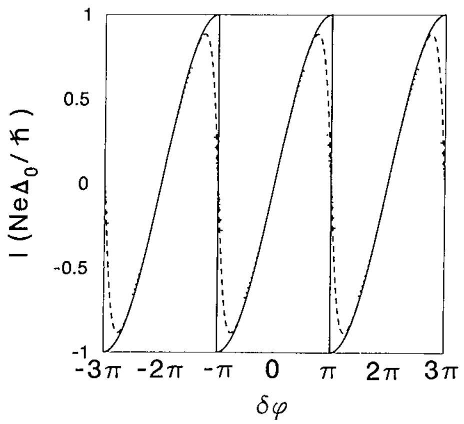

Fig. 8 Current–phase difference relation in a superconducting quantum point contact, much shorter than the coherence length, calculated from eq. (36) for three temperatures. Full line: $T = 0$. Dashed line: $T = 0.1\Delta_0/k_B$. Dotted line: $T = 0.2\Delta_0/k_B$. At these temperatures Δ_0 has approximately its zero-temperature value.

This is a good place to conclude our contribution to this symposium on analogies. The conductance quantization of a quantum point contact for electrons was discovered by surprise [12, 13]. The analogy with photons led to the prediction [9] and observation [10] of the discretized optical transmission cross-section of a slit. Now the notion of analogies has brought us the quantum point contact for Cooper pairs [1], with its discretized Josephson current. We hope that this paper will stimulate efforts to realize such a superconducting quantum point contact experimentally.

Acknowledgement

The authors acknowledge the support of M.F.H. Schuurmans.

References

[1] C.W J. Beenakker and H. van Houten, Phys. Rev. Lett 66 (1991) 3056.
[2] A. Furusaki, H. Takayanagi and M. Tsukada, Phys. Rev. Lett. 67 (1991) 132.
[3] P.C. van Son, Ph.D. Thesis, Nijmegen (1987).

[4] D Lenstra, in Studies in Mathematical Physics, Proc Huygens Symposium, eds E van Groesen and E M de Jager (North-Holland, Amsterdam) to be published
E C M van den Heuvel, Master Thesis, Eindhoven (1990)
[5] A F Andreev, Zh Eksp Teor Fiz 46 (1964) 1823, 49 (1965) 655 (Sov Phys JETP 19 (1964) 1228, 22 (1966) 455)
[6] B Ya Zel'dovich, V I Popovichev, VV Ragul'skii and F S Faizullov, Pis'ma Zh Eksp Teor Fiz 15 (1972) 160 (Sov Phys JETP 15 (1972) 109)
[7] A Yariv and R A Fisher, in Optical Phase Conjugation, ed R A Fisher (Academic Press, New York, 1983)
D M Pepper and A Yariv, in Optical Phase Conjugation, ed R A Fisher (Academic Press, New York, 1983)
[8] D Lenstra and W van Haeringen, in Analogies in Optics and Microelectronics, eds W van Haeringen and D Lenstra (Kluwer, Dordrecht, 1990)
[9] H van Houten and C W J Beenakker, in Analogies in Optics and Microelectronics, eds W van Haeringen and D Lenstra (Kluwer, Dordrecht, 1990)
[10] E A Montie, E C Cosman, G W 't Hooft, M B van der Mark and C W J Beenakker, Nature 350 (1991) 594
[11] A review of quantum transport in semiconductor nanostructures is C W J Beenakker and H van Houten, Solid State Physics 44 (1991) 1
[12] B J van Wees, H van Houten, C W J Beenakker, J G Williamson, L P Kouwenhoven, D van der Marel and C T Foxon, Phys Rev Lett 60 (1988) 848
[13] D A Wharam, T J Thornton, R Newbury, M Pepper, H Ahmed, J E F Frost D G Hasko, D C Peacock, D A Ritchie and G A C Jones, J Phys C 21 (1988) L209
[14] P G de Gennes, Superconductivity of Metals and Alloys (Benjamin, New York, 1966)
[15] J Bardeen, R Kummel, A E Jacobs and L Tewordt, Phys Rev 187 (1969) 556
[16] D M Pepper and R L Abrams, Optics Lett 3 (1978) 212
[17] J AuYeung, D Feteke, D M Pepper and A Yariv, IEEE J Quantum Electron QE-15 (1979) 1180
[18] A E Siegman, P A Belanger and A Hardy, in Optical Phase Conjugation, ed R A Fisher (Academic Press, New York, 1983)
[19] R Kummel, U Gunsenheimer and R Nicolsky, Phys Rev B 42 (1990) 3992
[20] S I Bozkho, V S Tsoi and S E Yakovlev, Pis'ma Zh Eksp Teor Fiz 36 (1982) 123 (JETP Lett 36 (1982) 153)
[21] P A M Benistant, H van Kempen and P Wyder Phys Rev Lett 51 (1983) 817
P A M Benistant, A P van Gelder, H van Kempen and P Wyder, Phys Rev B 32 (1985) 3351
[22] G E Blonder and M Tinkham, Phys Rev B 27 (1983) 112
[23] P C van Son, H van Kempen and P Wyder, Phys Rev Lett 59 (1987) 2226, Phys Rev B 37 (1988) 5015
[24] A Hahn, Phys Rev B 31 (1985) 2816
[25] P G de Gennes and D Saint-James Phys Lett 4 (1963) 151
[26] W L McMillan and P W Anderson, Phys Rev Lett 16 (1966) 85
[27] H Plehn, U Gunsenheimer and R Kummel, J Low Temp Phys , to be published
[28] A review of the Josephson effect in weak links is K K Likharev, Rev Mod Phys 51 (1979) 101
[29] H van Houten, Appl Phys Lett 58 (1991) 1326
[30] I O Kulik, Zh Eksp Teor Fiz 57 (1969) 1745 (Sov Phys JETP 30 (1970) 944)
[31] C Ishii, Prog Theor Phys 44 (1970) 1525
J Bardeen and J L Johnson, Phys Rev B 5 (1972) 72
A V Svidzinsky, T N Antsygina and E N Bratus', J Low Temp Phys 10 (1973) 131
G B Arnold J Low Temp Phys 59 (1985) 143
M Buttiker and T M Klapwijk, Phys Rev B 33 (1986) 5114
V Z Kresin, Phys Rev B 34 (1986) 7587
A Furusaki and H Takayanagi, Physica B 165 & 166 (1990) 967
B J van Wees, K -M H Lenssen and C J P M Harmans, Phys Rev B 44 (1991) 470
[32] P W Anderson, in Ravello-Lectures on the Many-Body Problem 2, ed E R Gianello (Academic Press, New York, 1963)
[33] C W J Beenakker and H van Houten, Proc Int Symp on Nanostructures and Mesoscopic Systems, ed W P Kirk (Academic Press, New York) to be published
[34] I O Kulik and A N Omel'yanchuk, Fiz Nisk Temp 3 (1977) 945, 4 (1978) 296 (Sov J Low Temp Phys 3 (1977) 459, 4 (1978) 142